Suppressing the Lattice Oxygen Release by Al-Doped in Li-Rich Mn-Based Layered Materials

Ziqi Xie [1], Hongjin Zhong [1], Zixuan Fang [1], Mengqiang Wu [1, *]

[1] School of Materials and Energy, University of Electronic Science and Technology of China , Chengdu ,611731, China

Abstract. Li-rich Mn-based layered materials (LRMs) are regarded as one of the most promising cathode materials due to their superior discharge specific-capacity. However, the irreversible lattice oxygen loss in LRMs at high voltages (＞4.5 V) leads to their poor structural stability and slow Li^+ diffusion kinetic. To solve these problems, this work successfully synthesized the Al-doped LRMs ($Li_{1.2}(Mn_{0.54}Ni_{0.13}Co_{0.13})_{1-x}Al_xO_2$ (x = 0, 0.01, 0.05, 0.1) by the hydrothermal method and subsequent high-temperature sintering. X-ray diffraction (XRD)， Scanning electron microscopy (SEM), and transmission electron microscopy (TEM) combined with the constant current charge-discharge tests effectively verified that Al doping effectively suppressed the irreversible lattice oxygen release and significantly improved the structural stability of LRMs.

Keywords： Lithium-ion battery, Li-Rich Mn-Based Layered Materials, Al doping, Lattice oxygen loss.

1. Introduction

Li-rich Mn-based layered materials (LRMs) can be represented by the formula $xLi_2MnO_3 \cdot (1-x)LiTMO_2$ (TM = Ni, Co, Mn, etc.).[1, 2] These materials have garnered significant attention due to their exceptionally high discharge specific capacity and energy density, as well as their relatively low cost.[3, 4] However, practical applications of LRMs are hindered by several challenges, such as the capacity and voltage degradation caused by lattice oxygen loss during the cycle.[5, 6] To address these issues, researchers have proposed various modification strategies, such as surface coating, lattice doping, and particle structure optimization in LRMs[7, 8].

Lattice doping, one of the most widely adopted modification strategies[9, 10], can effectively inhibit the migration of transition metal ions (TM^{n+}) and mitigate the irreversible lattice oxygen loss in LRMs during the cycle, thereby enhancing structural stability. And among all the dopants, Al^{3+} stands out due to its unique advantages.[11] Al^{3+} as an electrochemically inert cation that not only can play a "pinning effect" in the TM layer to alleviate the structural collapse, but also provide a strong Al-O bond inhibits irreversible lattice oxygen loss.

This study focuses on the structural and performance optimization of LRMs by Al doping, and successfully prepares Al-doped LRMs by the hydrothermal-assisted rapid nucleation method. Various characterization methods such as SEM, TEM, XRD, combined with constant current charge-discharge testing to revealed the mechanism, thereby providing certain theoretical support and technical paths for the research and development of LRMs with high energy density and long life.

2. Experimental

2.1 Material preparation

The stoichiometric ratio of $MnSO_4 \cdot H_2O$, $NiSO_4 \cdot 6H_2O$, $CoSO_4 \cdot 7H_2O$, and $Al(NO_3)_3 \cdot 9H_2O$ were dissolved in 25 mL of deionized water. Then, 12.5 mL of ethanol was added to the solution until no further bubbles were observed (designated as Solution A). Separately, $(NH_4)_2CO_3$ was weighed and dissolved in 25 mL of deionized water to prepare a colorless and transparent Solution B. Solution A and Solution B were mixed evenly and transferred to a hydrothermal reactor, where they were heated at 200 ℃ for 12 hours to obtain the precursor material ($(Mn_{0.675}Ni_{0.1625}Co_{0.1625})_{1-x}Al_xCO_3$, x=0,0.01, 0.05, and 0.1).

Subsequently, the precursor was weighed according to a molar ratio of 1:1.5 and mixed thoroughly with Li_2CO_3 in a mortar. The mixture was transferred to a muffle furnace and heated to 500 ℃ at a heating rate of 5 ℃/min for 3 hours. The temperature was then further increased to 800 ℃ at the same heating rate and maintained for 12 hours. After cooling to room temperature, the final product $Li_{1.2}(Mn_{0.54}Ni_{0.13}Co_{0.13})_{1-x}Al_xO_2$ can be obtained, as denoted as LR-Al-0, LR-Al-0.01, LR-Al-0.05, and LR-Al-0.1.

2.2 Material characterizations

The crystal structures of as-prepared materials were discussed by X-ray powder diffraction (XRD, Smart Lab 9000). The surface morphology and local crystal structures of samples were characterized by the Field emission scanning electron microscope (SEM, JSM-IT800) and transmission electron microscopy (TEM, JEOL JEM 2100 F).

2.3 Electrochemical measurements

Weigh the LRMs, Super P, and PVDF in a mass ratio of 8:1:1. Grind them thoroughly in a mortar, then add an appropriate amount of NMP to obtain a uniform fluid slurry. Subsequently, spread the slurry onto Al foil and dry at 120 ℃. Inside the glove box, assemble the battery components in the following sequence: positive electrode case, spring, gasket, lithium sheet, electrolyte, separator, additional electrolyte, electrode sheet, and negative electrode case. Finally, seal the battery using a battery packaging machine to obtain the finished product for subsequent electrochemical testing.

3. Results and discussion

Fig. 1a presents the XRD patterns of the prepared samples. All samples exhibited similar XRD patterns, indicating that Al doping had no effect on the crystal structure. The main peak positions align with the α-$NaFeO_2$ structure (R-3m space group), and a weak superlattice peak near 20°-25° reveals the presence of the Li_2MnO_3 phase (C/2m space group). In Fig. 1b, the (003) peak shifts to a lower angle compared to the pristine sample, confirming successful Al doped in LRMs. Moreover, the noticeable splitting peaks of the (006)/(102) and (018)/(110) in all samples reflects high order layered structure.

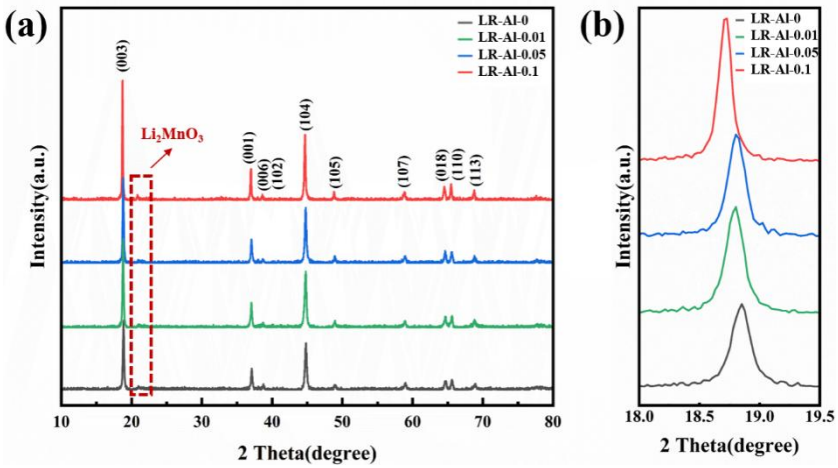

Fig.1 (a) XRD patterns; (b) Enlarged (003) peak of the prepared samples.

Fig. 2 shows the SEM image of the prepared sample. The spherical morphology of all samples was formed by the agglomeration of primary particles. Fig. 2a shows that the original sample presents a loose and porous morphology with a relatively low particle density. With the increase of Al doping content, the compactness of the particles rises, which can accelerate the Li^+ transport rate (Fig. 2b-d).

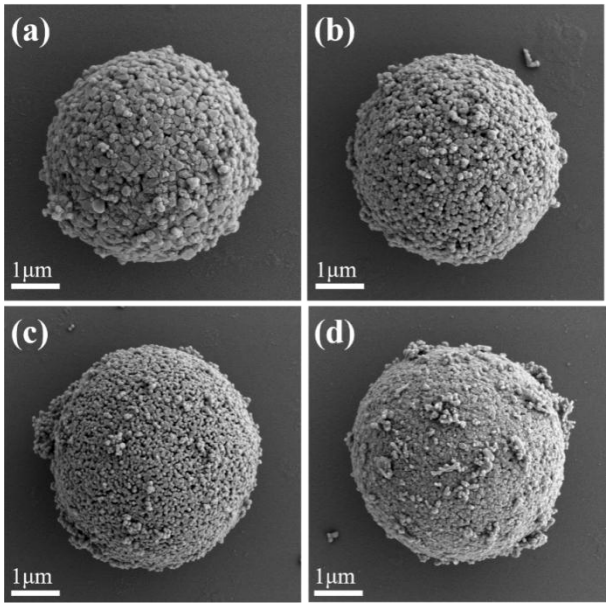

Fig.2 The SEM images of：(a) LR-AL-0；(b) LR-Al-0.01；
(c) LR-Al-0.05；(d) LR-Al-0.1samples.

TEM was used to further observe the effect of Al doping on the local crystal structure of as-prepared materials, as shown in Fig.3. All samples exhibited clear lattice fringes. The crystal plane spacings of the LR-Al-0, LR-Al-0.01, LR-Al-0.05 and LR-Al-0.1 samples were 0.475 nm, 0.479 nm, 0.480 nm and 0.481 nm respectively, corresponding to the (003) crystal plane. The increased interplanar spacing in LRMs is attributed to Al^{3+} doping, which can reduce the Li^+ transmission resistance, accelerate Li^+ transport rate, and thereby improve the rate performance of LRMs.

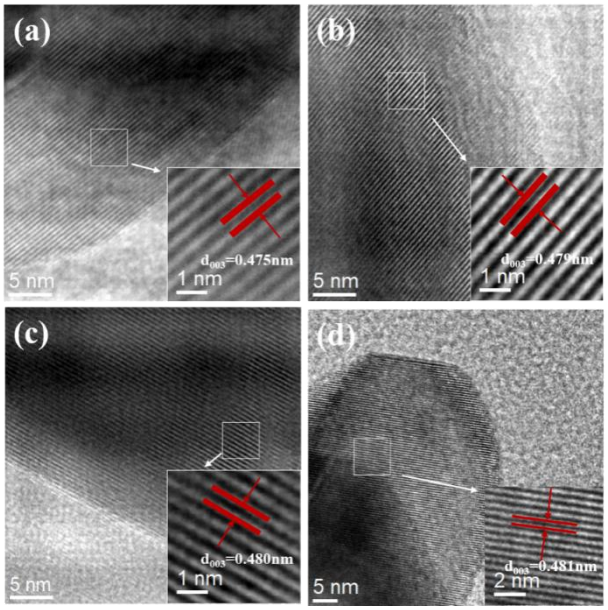

Fig.3 The TEM images of：(a) LR-AL-0；(b) LR-Al-0.01；
(c) LR-Al-0.05；(d) LR-Al-0.1 samples.

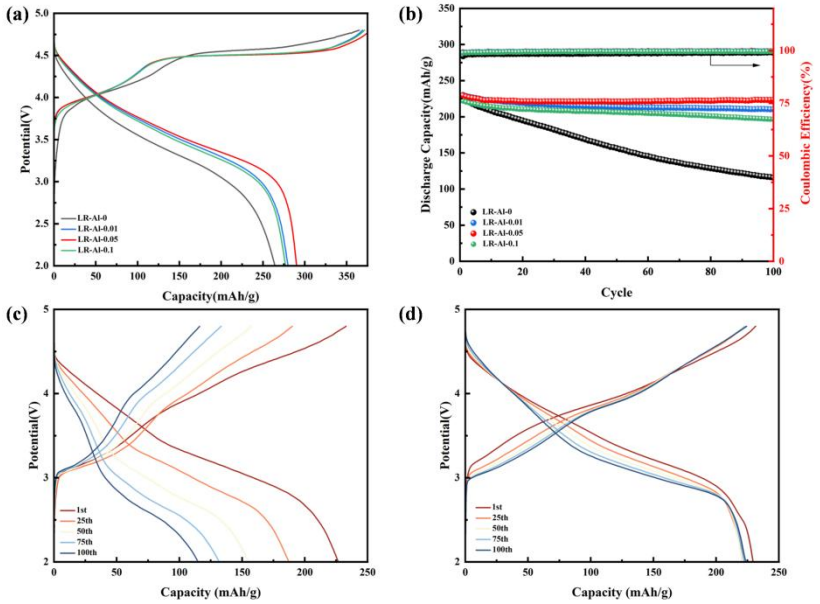

Fig. 4 (a) The initial charge/discharge curves of as-prepared materials vs. 2-4.8 V; (b) the cycle performance at 0.5 C; Selected charge/discharge profiles of the LR-Al-0 (c) and LR-Al-0.05 (d) samples at 0.5 C.

Fig. 4 shows the effect of Al doping on the electrochemical performance of LRMs. The initial discharge specific capacities of the LR-Al-0, LR-Al-0.01, LR-Al-0.05 and LR-Al-0.1 samples were 264.29 mAh/g, 279.93 mAh/g, 290.19 mAh/g, and 277.00 mAh/g at 0.1 C, and the corresponding initial Coulomb efficiencies were 72.37 %、77.13 %、77.39 %、74.57 % (Fig. 4a). Fig. 4b illustrates the cycling performance of as-prepared samples at 0.5 C. The initial discharge specific capacities of as-prepared samples at 0.5 C were 226.65 mAh/g, 232.22 mAh/g, 231.50 mAh/g, and 221.76 mAh/g, respectively. After 100 cycles, the discharge specific capacities were 115.49 mAh/g, 210.34

mAh/g, 223.53 mAh/g, and 196.51 mAh/g, corresponding the capacity retention rates were 51.04%, 90.58%, 96.56%, and 88.61%, respectively. In addition, the different charge-discharge curves were employed to evaluate the structural stability of LRMs during the cycle, as shown in Fig. 4c-d. The LR-Al-0.05 sample demonstrates a slight evolution of the charge-discharge curves, which can be attributed to the strong Al-O bond effectively inhibits the irreversible lattice oxygen loss, thereby enhancing the structural stability of LRMs.

4. Conclusion

The Al-doped LRMs were successfully prepared by the hydrothermal method, and the strong Al-O bond can effectively inhibit the irreversible lattice oxygen loss, thereby improving the structural stability of LRMs. Furthermore, the Al doping mechanism was deeply explored through XRD, SEM and TEM combined with constant current charge-discharge tests. After modification, the Al-doped LRMs exhibited excellent electrochemical performance, the capacity retention rate was 96.56% after 100 cycles at 0.5 C.

Acknowledgments

This work was financially supported by the Natural Science Foundation of Sichuan Province (Grant No.2025NSFSC0100), the Sichuan Major Science and Technology Department Program (Grant No.2024ZHCG0150), and the Sichuan Science and Technology Department Program (Grant No.2023ZHJY0019).

References

[1] ZHANG M, LI J, PANG Q, et al. Phase Transition Behavior During Sintering Process of Li-Rich Materials [J]. Advanced Energy Materials, 2025, 15(21), 2406031.

[2] YANG M, CHEN T, WANG G, et al. A Surface-to-Interface Boronation Engineering Strategy Stabilizing the O/Mn Redox Chemistry of Lithium-Rich Manganese based Oxides towards High Energy-Density Cathodes [J]. Energy & Environmental Science, 2025, 04857.

[3] MCCOLL K, COLES S W, ZARABADI-POOR P, et al. Phase segregation and nanoconfined fluid O2 in a lithium-rich oxide cathode [J]. Nature Materials, 2024, 23(6): 826-833.

[4] SAROHA R, CHO J S, AHN J-H. Synergetic effects of cation (K+) and anion (S2−)-doping on the structural integrity of Li/Mn-rich layered cathode material with considerable cyclability and high-rate capability for Li-ion batteries [J]. Electrochimica Acta, 2021, 366, 137471.

[5] TU J, LI Y, ZHANG B, et al. Strategies toward high-energy-density Co-free lithium nickel manganese oxide: from crystal structure control to flexible configuration design [J]. Energy & Environmental Science, 2025, 18(9): 4010-4036.

[6] WANG L, XU L, XUE W, et al. Synergistic enhancement of Li-rich manganese-based cathode materials through single crystallization and in-situ spinel coating [J]. Nano Energy, 2024, 121, 109241.

[7] LI J-C, TANG J, TIAN J, et al. From Oxygen Redox to Sulfur Redox: A Paradigm for Li-Rich Layered Cathodes [J]. Journal of the American Chemical Society, 2024, 146(11): 7274-7287.

[8] CHENG W, DING J, LIU Z, et al. Zn/Ti dual concentration-gradients surface doping to improve the stability and kinetics for Li-rich layered oxides cathode [J]. Chemical Engineering Journal, 2023, 451, 138678.

[9] XIE Z, ZHANG M, LI Y, et al. Enhanced the diffusion kinetics and cycle stability of Li-rich layered materials by introducing the Li-O-Al configuration and robust Nb-O bonds [J]. Chemical Engineering Journal, 2025, 505, 159630.

[10] WANG G, XIE C, WANG H, et al. Mitigated Oxygen Loss in Lithium-Rich Manganese-Based Cathode Enabled by Strong Zr–O Affinity [J]. Advanced Functional Materials, 2024, 34(23), 2313672.

[11] WANG E, XIAO D, WU T, et al. Al/Ti Synergistic Doping Enhanced Cycle Stability of Li-Rich Layered Oxides [J]. Advanced Functional Materials, 2022, 2201744.